NIR spectroscopy of selected iron(II) and iron(III) sulphates

Ray L. Frost •, Rachael-Anne Wills, Wayde Martens, Matt Weier, and B. Jagannadha Reddy

Inorganic Materials Research Program, School of Physical and Chemical Sciences, Queensland University of Technology, GPO Box 2434, Brisbane Queensland 4001, Australia.

This is the authors' version of a paper that was later published in:

(2005) Spectrochimica Acta 62(1):pp. pp42-50.

Abstract

A problem exists when closely related minerals are found in paragenetic relationships. The identification of such minerals cannot be undertaken by normal techniques such as X-ray diffraction. Vibrational spectroscopic techniques may be applicable especially when microtechniques or fibre-optic techniques are used. NIR spectroscopy is one technique which can be used for the identification of these paragenetically related minerals and has been applied to the study of selected iron(II) and iron(III) sulphates. The Near–IR spectral regions may be conveniently divided into four regions (a) the high wavenumber region > 7500 cm^{-1} (b) the high wavenumber region between 6400 and 7400 cm^{-1} attributed to the first overtone of the fundamental hydroxyl stretching mode (c) the 5500-6300 cm^{-1} region attributed to water combination modes of the hydroxyl fundamentals of water, and (d) the 4000-5500 cm^{-1} region attributed to the combination of the stretching and deformation modes of the iron(II) and iron(III) sulphates. The minerals containing iron(II) show a strong, broad band with splitting, around 11000-8000 cm^{-1} attributed to $^5T_{2g} \rightarrow {}^5E_g$ transition. This shows the ferrous ion has distorted octahedral coordination in some of these sulphate minerals. For each of these regions, the minerals show distinctive spectra which enable their identification and characterisation. NIR spectroscopy is a less used technique which has great application for the study of minerals, particularly minerals which have hydrogen in the structure either as hydroxyl units or as water bonded to the cation as is the case for iron(II) and iron(III) sulphates. The study of minerals on planets is topical and NIR spectroscopy provides a rapid technique for the distinction and identification of iron(II) and iron(III) sulphates minerals.

Keywords: iron(II) sulphates**,** coquimbite, jarosite, romerite, iron(III) sulphates, melanterite, siderotil, near-IR spectroscopy

Introduction

• Author to whom correspondence should be addressed (r.frost@qut.edu.au)

Interest in the study of iron(II) sulphates arises from at least two perspectives. Firstly the observation of sulphates of iron on Mars by recent exploration and secondly by the formation of iron(II) and iron(III) sulphates in evaporate deposits [1]. Studies of these minerals have been undertaken for some considerable time [2-6].

Near IR spectroscopy provides a suitable method for the analysis of these types of materials [7-10]. The other use of near-IR spectroscopy is in the search for knowledge of minerals in the solar system [11-16]. Hunt et al. first applied NIR spectroscopy to the study of minerals [17, 18]. It should be recognised that Near-IR spectroscopy is known also as proton spectroscopy such that this type of spectroscopy is most useful for measuring bonds involving hydrogen such as OH, NH, CH etc. Thus the technique appears most suitable for the measurement of hydrated, hydroxylated sulphates as might be found in soils and sediments that may exist on Mars. The Mars mission rover known as opportunity has been used to discover the presence of jarosite on Mars, thus providing evidence for the existence or pre-existence of water on Mars.
(http://www.news.cornell.edu/releases/rover/Mars.jarosite.html)
Recent studies have identified iron sulphate minerals on Mars [19-22].

Six distinct iron(II) sulphates are known to occur naturally. These are melanterite ($FeSO_4.7H_2O$) [23-25], its polymorph tauriscite, ferrohexahydrite ($FeSO_4.6H_2O$), siderotil ($FeSO_4.5H_2O$) [26-28]; rozenite ($FeSO_4.4H_2O$) [29, 30]; and szomolnokite ($FeSO_4.H_2O$) [26, 31]. There are a large number of iron(III) sulphate minerals. There are some 43 in total iron(III) sulphates. There is a comprehensive listing in the text 'Oxide Zone Geochemistry by Peter Williams Table 9.4 [32]. These include coquimbite $(Fe^{3+})_2(SO_4)_3.9H_2O$ [2, 25, 33-35]; jarosite $KFe_3(SO_4)_2(OH)_6$ where the K may be replaced by Na, Pb, Ag or $(NH_4)^+$ [36-38]; romerite, a mixed iron(II)/iron(III) sulphate $Fe^{2+}(Fe^{3+})_2(SO_4)_4.14H_2O$; and parabutlerite $FeSO_4.(OH).2H_2O$ [2, 39-41].

Thermal emission studies have been used to study minerals on Mars or at least to mimic possible models of Martian minerals [42-45]. Some studies attempt to model the possible equilibria of minerals such as the iron sulphates in an attempt to predict the geochemical evolution of Martian minerals [46]. This model proposes five stages of evolution of Martian minerals. The formation of iron(II) and iron(III) sulphates are included in this model. Such formation based upon chemical equilibria must include concentrated solutions and the effect of pH, temperature and other factors. Such equilibria are complex to say the least [47, 48]. One effective method of studying hydrated and hydroxylated minerals is to use NIR spectroscopy. The existence of iron(II) and iron(III) sulphate minerals would confirm the existence/pre-existence of water on Mars. The advantages of NIR spectroscopy include remote sensing, sensitivity to minerals containing OH and NH groups and the ease of operation of the technique.

In order to determine the presence of specific minerals on planets such as Mars or the moons of Saturn using NIR spectroscopy, it is necessary to build a data base of NIR spectra of minerals. Recent exploration of Mars has indicated using Mossbauer Spectroscopy the presence of iron minerals such as hematite which has formed in small nodules. Such secondary minerals can be formed from solution. This of course is an indication of the pre-existence of water on Mars. Not only should the

data base contain natural minerals i.e. earth stable structures but also unstable structures since both the physical and chemical conditions on planets may be very different to the conditions on earth. The technique of NIR spectroscopy is very relevant to the study of minerals on planets such as Mars since the miniaturisation of the technology is possible. In this research we report the NIR spectroscopy of selected iron(II) and iron(III) sulphates.

Experimental

Minerals

The minerals used in this research are shown in Table 1. Since there are many iron(III) and at least six known simple iron(II) sulphates, a selection of minerals was made. Many of the minerals used in this study are 'type' minerals. They have been analysed by X-ray diffraction for phase identification and the minerals have been analysed by electron microprobe analysis for composition.

Near-infrared spectroscopy (NIR)

Near IR spectra were collected on a Nicolet Nexus FT-IR spectrometer with a Nicolet Near-IR Fibreport accessory. A white light source was used, with a quartz beam splitter and TEC NIR InGaAs detector. Spectra were obtained from 11 000 to 4000 cm^{-1} by the co-addition of 64 scans at a resolution of 8cm^{-1}. A mirror velocity of 1.266 m/sec was used. The spectra were transformed using the Kubelka-Munk algorithm to provide spectra for comparison with absorption spectra.

Spectral manipulation such as baseline adjustment, smoothing and normalisation were performed using the Spectracalc software package GRAMS (Galactic Industries Corporation, NH, USA). Band component analysis was undertaken using the Jandel 'Peakfit' software package which enabled the type of fitting function to be selected and allows specific parameters to be fixed or varied accordingly. Band fitting was done using a Lorentz-Gauss cross-product function with the minimum number of component bands used for the fitting process. The Gauss-Lorentz ratio was maintained at values greater than 0.7 and fitting was undertaken until reproducible results were obtained with squared correlations of r^2 greater than 0.995.

Results and discussion

The Near–IR spectral regions may be conveniently divided into four regions (a) the high wavenumber region > 7500 cm^{-1} (b) the high wavenumber region between 6400 and 7400 cm^{-1} attributed to the first overtone of the fundamental hydroxyl stretching mode (c) the 5500-6300 cm^{-1} region attributed to water combination modes of the hydroxyl fundamentals of water, and (d) the 4000-5500 cm^{-1} region attributed to the combination of the stretching and deformation modes of the iron(II) and iron(III) sulphates. The NIR spectra in the 5350 to 7350 cm^{-1} region of parabutlerite, romerite, ferricopiapite, jarosite and coquimbite are shown in Figure 1. These spectra combine the regions b and c delineated above as the two spectral regions overlap for the iron(III) sulphates. Figure 2 displays the NIR spectra of the

iron(II) sulphates melanterite and siderotil. The spectral analyses of the data of the iron(II) and iron(III) sulphates are reported in Tables 2 and 3 respectively.

The spectral region in the 6400 to 7400 cm^{-1} region shows the first fundamental overtone of the OH stretching vibration. A number of conclusions can be readily made: (a) the NIR spectra of the iron(II) sulphates melanterite and siderotil are very similar in the region of the first fundamental; (b) the spectra of the iron(III) sulphates are different in this wavenumber region; (c) the spectra of the iron(III) sulphates are different from the iron(II) sulphates. The iron(III) mineral coquimbite ($(Fe^{3+})_2(SO_4)_3.9H_2O$) is characterised by overlap of the first HOH fundamentals and the HOH combination bands. This mineral shows intense bands at 6918 and 6646 cm^{-1} (Table 2a). The spectral pattern for the iron(II) minerals is different. The mineral melanterite ($FeSO_4.7H_2O$) is characterised by intense bands at 6926, 6396 and 6763 cm^{-1} (Table 3). The iron(II) mineral siderotil shows a similar spectrum but with additional resolved bands at 6178 and 6932 cm^{-1}. The mixed iron(II)/(III) mineral romerite ($Fe^{2+}(Fe^{3+})_2(SO_4)_4.14H_2O$) shows bands at 6416, 6857, 6938 and 7042 cm^{-1}(Table 2b). The iron(III) mineral ferricopiapite ($((Fe^{3+})_{2/3}(Fe^{3+})_4(SO_4)_6(OH)_2.20H_2O$) has NIR bands in this spectral region at 6984, 6892, 6758 and 6586 cm^{-1}. The NIR spectra of two samples of the mineral jarosite ($KFe_3(SO_4)_2$) from different origins in the 5350 to 7350 cm^{-1} region are different. The first jarosite sample m30720 is the potassium jarosite whereas the sample m32767 is a lead jarosite. The difference in the spectra shows that jarosites with different cations can be distinguished. These data show that these iron(II) and iron(III) sulphates may be distinguished and characterised by their NIR spectra in this spectral region.

The NIR spectra in the 4000 to 5500 cm^{-1} region for the iron (III) and iron(II) sulphate minerals are shown in Figures 3 and 4 respectively. The two iron(II) minerals melanterite and siderotil show strong similarity in this spectral region. There are differences in intensity over the 4000 to 4500 cm^{-1} range. NIR bands are observed at 5156, 5125, 5046, 4991, 4815, 4584, 4180 and 4102 cm^{-1} for siderotil and 5153, 5124, 5043, 5023, 4799, 4578, 4212 and 4127 cm^{-1} for melanterite. Slight shifts in the band positions are observed which may be useful for distinguishing between the two iron(II) minerals. The spectra of siderotil and melanterite do show some resemblance to the spectrum of coquimbite. NIR bands are observed for coquimbite at 5214, 5144, 5066, 5010 and 4838 cm^{-1}. The NIR spectrum of the mineral ferricopiapite is different from the other iron(II) and iron(III) minerals. NIR bands of ferricopiapite are found at 5288, 5155, 5065, 4974, 4724 and 4538 cm^{-1}. The minerals romerite and parabutlerite show a broad profile over the 4400 to 5200 cm^{-1} region. For romerite bands are observed at 5208, 5134, 5058, 4966, 4945, 4770, 4613, 4538 and 4462 cm^{-1}. Other lower intensity bands are observed in the 4000 to 4100 cm^{-1} region.

The high wavenumber region (7500-1100 cm^{-1}) of the iron(II) and iron(III) sulphates are shown in Figures 5 and 6 respectively. This region shows in-part the electronic spectra of the minerals. For most iron(II) minerals an intense NIR band is observed centered around 9500 cm^{-1}. Iron(III) minerals normally show no bands in this spectral region. Thus the NIR spectra in this region for coquimbite and ferricopiapite as shown in Figure 6 are correct. Minerals such as romerite do contain Fe(II) and so their spectra display bands in this region.

Iron is the most common transition element in minerals. For all transition elements, unfilled d orbitals have identical energies in an isolated ion, but the energy levels split when the ion is located in a crystal field. The energy levels are determined by the valence state of the atom (e.g. Fe^{2+}, Fe^{3+}), its coordination number, and the symmetry of the site it occupies [49]. In the present investigations of the electronic spectra of some selected iron(II) sulphate minerals in the near IR spectral features are simply due to the ferrous ion. So theory is now presented briefly to explain the spectral properties of the ferrous ion. The ferrous ion has an electronic structure, $(A)3d^6$. In an octahedral crystal field (O_h) it gives rise to $^5T_{2g}$, ^5E_g, ^3E_g and $^3T_{2g}$ states along with some more triplets and singlets. Of these, $^5T_{2g}$ forms the ground state. The only spin allowed transition is $^5T_{2g} \rightarrow {}^5E_g$ which shows a strong band for all ferrous ion complexes where as the remaining transitions are spin forbidden and they are generally weak bands. The ^5E_g state is unstable and is influenced by Jahn-Teller effect.

The NIR spectra of the samples are depicted in Figures 5 and 6. Interestingly, all the minerals under study show a strong, broad band with splitting, around 11000-8000 cm^{-1} except the minerals coquimbite and ferricopiapite. This is the characteristic broad band observed with two component bands by a separation of the order of 1000 cm^{-1} in several complexes [50-52]. A number of components are observed when the component bands are resolved. Therefore, the broad band with two main component bands is attributed to $^5T_{2g} \rightarrow {}^5E_g$ transition. The average of these two bands is 10Dq and separation between them gives the nature of distortion [53-56]. The splitting of the $^5T_{2g} \rightarrow {}^5E_g$ band for the minerals presented in the Table 4 shows that the amount of splitting is more in m34345 siderotil which implies distortion is more in this complex than the other minerals. The ferrous ion has distorted octahedral coordination in the sulphate minerals studied.

Conclusions

Near-IR spectroscopy is a technique, which has not been previously applied in depth to the study of iron(III) and iron(II) sulphates. Indeed iron(III) and iron(II) sulphates by their very nature, being composed of coordinated water and hydroxyl units coordinated to either the Fe(II) or Fe(III) ion, lend themselves to study by NIR. NIR reflectance techniques have proven most useful for the analysis of iron(III) and iron(II) sulphates.

A number of conclusions are made:

a. Iron (II) and iron (III) sulphates may be distinguished by the NIR high wavenumber region around 10,0000 cm^{-1}.
b. NIR of iron(III) sulphates showing bands at 10,000 cm^{-1} also contain some iron(II).
c. The splitting of the 10,000 cm^{-1} band provides an indication of the distortion of the octahedral symmetry of the Fe^{2+} ion.
d. NIR spectroscopy of the first fundamental overtone can be used to distinguish between hydrated and hydroxylated iron(II) and iron(III) sulphates.
e. NIR spectroscopy of the first fundamental overtone can be used to distinguish between hydrated and hydroxylated iron(III) sulphates.

NIR spectroscopy shows that the spectra of iron(II) and iron(III) sulphates in the water HOH first fundamental overtone and combination regions are different. This difference suggests that the structure of water around the cations is different between the different iron(II) and iron(III) sulphate minerals. The structural arrangement of the water molecules in the mineral is sample dependent. NIR spectroscopy has the ability to distinguish between iron(III) and iron(II) sulphates even when the formula of the minerals is closely related. The NIR spectroscopic technique has great potential as a mineral exploratory tool on planets and in particular Mars.

Acknowledgments

The financial and infra-structure support of the Queensland University of Technology Inorganic Materials Research Program of the School of Physical and Chemical Sciences is gratefully acknowledged. The Australian Research Council (ARC) is thanked for funding. One of the authors (BJR) thanks The Queensland University of Technology for a Visiting Professorship.

The authors wish to thank and gratefully acknowledge the support of Mr Dermot Henry of Museum Victoria for the loan of the minerals used in this study.

References

[1]. T. Buckby, S. Black, M. L. Coleman and M. E. Hodson, Min. Mag. 67 (2003) 263.
[2]. F. Cesbron, Bull. Soc. Franc. Mineral. Crist. 87 (1964) 125.
[3]. W. H. Baur, Fortschritte der Mineralogie 39 (1961) 333.
[4]. E. G. Ehlers and D. V. Stiles, Amer. Miner. 50 (1965) 1457.
[5]. R. Scharizer, Zeitschrift fuer Kristallographie und Mineralogie 43 (1907) 113.
[6]. R. Scharizer, Zeitschrift fuer Kristallographie und Mineralogie 46 (1909) 427.
[7]. M. Long and S.-Q. Pei, Yankuang Ceshi 22 (2003) 169.
[8]. C. A. Russell, Com. Soil Sc. Plant Anal. 34 (2003) 1557.
[9]. J. W. Van Groenigen, C. S. Mutters, W. R. Horwath and C. Van Kessel, Plant and Soil 250 (2003) 155.
[10]. C.-W. Chang, D. A. Laird, M. J. Mausbach and C. R. Hurburgh, Jr., Soil Sci. Soc. of Amer. J. 65 (2001) 480.
[11]. I. Biering, K. Larsen, T. Garp, D. H. Christensen, C. B. Koch, P. W. Jensen and O. F. Nielsen, Asian Chem. Letts. 7 (2003) 99.
[12]. T. H. Burbine and R. P. Binzel, Icarus 159 (2002) 468.
[13]. C. D. Cooper and J. F. Mustard, Icarus 158 (2002) 42.
[14]. N. Hirao, Ganseki Kobutsu Kagaku 31 (2002) 111.
[15]. L. A. Mcfadden, D. D. Wellnitz, M. Schnaubelt, M. J. Gaffey, J. F. Bell, Iii, N. Izenberg, S. Murchie and C. R. Chapman, Meteoritics & Planet. Sc. 36 (2001) 1711.
[16]. G. Bellucci, Earth, Moon, and Planets 78 (1999) 305.
[17]. G. R. Hunt and R. C. Evarts, Geophys. 46 (1981) 316.
[18]. G. R. Hunt and R. P. Ashley, Econ. Geol. and Bull. Soc. Econ. Geol. 74 (1979) 1613.
[19]. J.-P. Bibring, Y. Langevin, F. Poulet, A. Gendrin, B. Gondet, M. Berthe, A. Soufflot, P. Drossart, M. Combes, G. Bellucci, V. Moroz, N. Mangold and B. Schmitt, Nature 428 (2004) 627.
[20]. M. E. Elwood Madden, R. J. Bodnar and J. D. Rimstidt, Nature 431 (2004) 821.
[21]. M. E. E. Madden, R. J. Bodnar and J. D. Rimstidt, Nature 431 (2004) 821.
[22]. D. T. Vaniman, D. L. Bish, S. J. Chipera, C. I. Fialips, J. William Carey and W. C. Feldman, Nature 431 (2004) 663.
[23]. A. A. Olowe and J. M. R. Genin, Hyperfine Interacts 68 (1992) 253.
[24]. S. N. Reddy, P. S. Rao, R. V. S. S. N. Ravikumar, B. J. Reddy and Y. P. Reddy, Spec. Acta, 57A (2001) 1283.
[25]. J. N. Thomas, P. D. Robinson and J. H. Fang, Am. Min. 59 (1974) 582.
[26]. R. D. Cody and D. L. Biggs, Can. Min. 11 (1973) 958.
[27]. J. L. Gooding, Icarus 33 (1978) 483.
[28]. J. L. Jambor and R. J. Traill, Can. Min. 7 (1963) 751.
[29]. J. Kubisz, Bull. acad. polon. sci., Ser. sci., Chim., geol. et geograph. 8 (1960) 107.
[30]. J. Kubisz, Przeglad Geologiczny 17 (1969) 582.
[31]. J. Kubisz, Bull. acad. polon. sci., Ser. sci., Chim., geol. et geograph. 8 (1960) 101.
[32]. P. A. Williams, *Oxide Zone Geochemistry*, Ellis Horwood Ltd, Chichester, West Sussex, England, 1990.

[33]. J. H. Fang and P. D. Robinson, Neues Jahrbu. Min., Monatshefte (1974) 89.
[34]. C. Giacovazzo, S. Menchetti and F. Scordari, Atti della Accademia Nazionale dei Lincei, Classe di Scienze Fisiche, Matematiche e Naturali, Rendiconti 49 (1970) 129.
[35]. A. Kovacs, Foldtani Kozlony 127 (1998) 353.
[36]. H. H. Adler and P. F. Kerr, Can. Min. 50 (1965) 132.
[37]. E. B. Burgina, G. N. Kustova, S. G. Nikitenko, D. I. Kochubey and G. L. Elizarova, Zhurnal Strukturnoi Khimii 37 (1996) 275.
[38]. K. Omori and P. F. Kerr, Geol. Soc. Am. Bull. 74 (1963) 709.
[39]. L. F. Aristarain, Revista del Museo Argentino de Ciencias Naturales 1 (1999) 145.
[40]. J. Borene, Bull. Soc. Franc. Mineral. Cristall. 93 (1970) 185.
[41]. S. V. Gevork'yan and A. S. Povarennykh, Mineralogicheskii Zhurnal 2 (1980) 33.
[42]. J. R. Michalski, M. D. Kraft, T. Diedrich, T. G. Sharp and P. R. Christensen, Geophys.Res. Letts. 30 (2003) PLA2/1.
[43]. D. L. Bish, J. William Carey, D. T. Vaniman and S. J. Chipera, Icarus 164 (2003) 96.
[44]. M. D. Lane and P. R. Christensen, Icarus 135 (1998) 528.
[45]. R. L. Huguenin, J. Geophys. Res. 79 (1974) 3895.
[46]. G. M. Marion, D. C. Catling and J. S. Kargel, Geochim. Cosmochim. Acta 67 (2003) 4251.
[47]. F. K. Cameron, J. Phys. Chem. 34 (1930) 692.
[48]. E. Posnjak and H. E. Merwin, J. Am. Chem. Soc. 44 (1922) 1965.
[49]. R. G. Burns, *Mineralogical Applications of Crystal Field Theory (Cambridge Earth Sciences Series)*, 1970.
[50]. G. R. Rossman and M. N. Taran, Am. Min. 86 (2001) 896.
[51]. A. V. Chandrasekhar, M. V. Ramanaiah, B. J. Reddy, Y. P. Reddy, P. S. Rao and R. V. S. S. N. Ravikumar, Spec. Acta, 59A (2003) 2115.
[52]. S. N. Reddy, P. S. Rao, R. V. Ravikumar, B. J. Reddy and Y. P. Reddy, Spec. acta. 57A (2001) 1283.
[53]. A. S. Marfunin, Probl. Kristallokhim. Miner. Endog. Mineraloobraz. (1967) 29.
[54]. A. S. Marfunin, R. M. Mineeva, A. R. Mkrtchyan, Y. M. Nyussik and V. E. Fedorov, Izvestiya Akademii Nauk SSSR, Seriya Geologicheskaya (1967) 86.
[55]. A. S. Marfunin, *Spectroscopy, Luminescence, and Radiation Centers in Minerals*, 1979.
[56]. A. S. Marfunin, A. R. Mkrtchyan, G. N. Nadzharyan, Y. M. Nyussik and A. N. Platonov, Izvestiya Akademii Nauk SSSR, Seriya Geologicheskaya (1971) 87.

Table 1 List of minerals, their Museum Victoria numbers and their origin

Mineral	Museum Id Number	Chemical Formula	Origin
Iron(II) sulphates			
Melanterite	M422	$FeSO_4.7H_2O$	Australia, Victoria, Ringwood (37 49 S, 145 14 E)
Siderotil	M 34345	$FeSO_4.5H_2O$	New Zealand, New Caledonia Mine, Thames
Iron(III) sulphates			
Coquimbite	M 30091	$(Fe^{3+})_2(SO_4)_3.9H_2O$	Dexter Mine, Utah, USA
Ferricopiapite	M 37054	$((Fe^{3+})_{2/3}(Fe^{3+})_4(SO_4)_6(OH)_2.20H_2O)$	Queensland, 4th level, Mt Isa Mine, Mt Isa
Parabutlerite	M47134	$FeSO_4.(OH).2H_2O$	Iran, Yazd province, Yazd
Romerite	M 37059	$Fe^{2+}(Fe^{3+})_2(SO_4)_4.14H_2O$	Queensland, 4th level, Mt Isa Mine, Mt Isa
Jarosite (K)	M 30720	$KFe_3(SO_4)_2(OH)_6$	Australia, South Australia, Brukunga, Shepherd Hill quarry (35 00 S, 138 58 E)
Jarosite (Pb) Plumbojarosite	M 32767	$PbFe_6(SO_4)_4(OH)_{12}$	Mexico, Lamode Toro Mine

Table 2a Table of NIR spectral results of selected iron(III) sulphate minerals

m30091 Coquimbite			m30720 Jarosite			m32767 Jarosite		
Center	FWHM	Area	**Center**	FWHM	Area	**Center**	FWHM	Area
						10735	302.3	0.015
						10269	655.0	0.188
			10232	975.3	0.265			
						9846	446.3	0.079
						8990	253.4	0.002
						8480	331.4	0.005
						7735	644.2	0.007
						7292	123.2	0.001
7062	97.7	0.003						
6918	248.2	0.049						
6887	61.1	0.004						
						6856	163.2	0.077
			6806	88.4	0.029	**6806**	75.9	0.015
						6664	175.2	0.021
6646	492.7	0.091						
			6565	331.7	0.044			
						6536	144.9	0.018
						6347	104.2	0.002
6056	570.0	0.062						
						5880	291.5	0.027
5744	396.5	0.048						
						5670	206.2	0.023
						5530	143.4	0.018
			5410	60.4	0.024	**5409**	65.5	0.024
			5363	38.6	0.007	**5365**	44.4	0.008
5214	102.7	0.060						
						5181	118.0	0.013
5144	91.3	0.072						
			5133	221.6	0.013			
						5097	108.0	0.086
5066	95.0	0.030						
5010	228.3	0.131				**5005**	93.4	0.019
4838	352.3	0.067						
			4810	271.2	0.014	**4811**	387.3	0.208
						4585	148.5	0.044
			4525	230.9	0.213			
			4505	71.9	0.020	**4509**	85.2	0.031
						4426	47.3	0.018
			4410	64.2	0.085			
						4395	52.2	0.022
			4347	39.1	0.024	**4349**	34.5	0.003
						4293	39.0	0.002
						4263	20.9	0.000
			4158	96.8	0.102			
4096	256.2	0.094						

			4065.1	64.2	0.032			
4017	4.9	0.001	**4012.6**	91.9	0.070			

Table 2b Table of NIR spectral results of selected iron(III) sulphate minerals

m37054 Ferricopiapite			m37059 Romerite			m47134 Parabutlerite		
Center	FWHM	Area	**Center**	FWHM	Area	**Center**	FWHM	Area
						10471	683.6	0.011
			9902	526.0	0.019			
						9891	567.0	0.172
			9101	974.5	0.077			
						8544	439.8	0.033
			8498	703.8	0.074			
			7042	116.5	0.011			
6984	149.8	0.025						
			6938	123.8	0.029			
6892	120.4	0.039						
			6857	77.5	0.003			
6758	197.6	0.041						
6586	185.7	0.009						
			6416	207.3	0.013			
			6181	340.3	0.080			
5998	242.3	0.013						
						5972	613.3	0.253
			5870	327.5	0.084			
5769	284.4	0.037						
			5682	230.2	0.048			
5574	163.1	0.010						
			5546	152.9	0.016			
5228	98.8	0.032						
			5208	134.7	0.072			
5155	92.6	0.123						
			5134	156.2	0.073			
						5113	145.0	0.125
5065	113.0	0.063	**5058**	187.3	0.036			
4974	283.8	0.108	**4966**	213.9	0.066			
			4945	228.5	0.014	**4960**	227.5	0.104
						4861	122.2	0.027
			4770	235.0	0.061			
4724	241.3	0.035				**4736**	155.8	0.068
			4613	152.2	0.018	**4615**	84.9	0.011
						4568	19.9	0.002
4538	91.2	0.007	**4538**	107.5	0.012			
						4492	8.0	0.000
						4481	13.1	0.001
			4462	71.8	0.007	**4465**	12.2	0.001
						4452	15.7	0.003
						4434	19.1	0.003
						4414	29.0	0.010
						4401	9.4	0.001
						4387	11.9	0.002
						4372	22.1	0.007
						4345	26.0	0.005

						4315.4	12.1	0.001
			4298.4	11.9	0.001			
			4281.4	15.0	0.001	**4282.1**	11.9	0.001
						4237.8	13.5	0.002
			4261.1	31.2	0.002			
			4241.9	19.5	0.002			
			4228.8	13.0	0.002	**4222.3**	13.6	0.003
			4213.9	11.4	0.001	**4205.4**	16.0	0.003
						4193.2	10.0	0.002
			4176.6	47.5	0.015	**4183.3**	13.2	0.003
						4168.0	18.6	0.006
4144.5	11.0	0.001				**4149.1**	9.8	0.001
4142.7	190.2	0.114						
						4136.6	97.9	0.000
4121.7	8.7	0.001						
4102.1	12.9	0.002						
4089.3	8.5	0.002						
4070.5	24.6	0.007						
4058.6	8.5	0.002						
4046.7	19.9	0.007						
4036.4	9.3	0.004						
4026.3	11.0	0.005						
4015.3	9.0	0.004						
4005.6	22.5	0.006						

Table 3 NIR data of iron(II) sulphates

m34345 Siderotil			m422 Melanterite		
Center	FWHM	Area	**Center**	FWHM	Area
10648	392.1	0.005			
10150	898.7	0.076			
9173	1225.9	0.152			
8425	786.8	0.068			
7989	490.7	0.016			
6932	224.3	0.028			
6923	76.9	0.002	**6926**	183.6	0.028
6756	307.5	0.039	**6763**	341.8	0.050
6447	387.0	0.024			
			6396	447.6	0.029
6178	251.8	0.005			
5156	146.6	0.127	**5153**	145.9	0.121
5125	68.5	0.022	**5124**	48.3	0.007
5046	100.8	0.062	**5043**	86.3	0.033
			5023	281.9	0.118
4991	224.1	0.062			
4815	268.3	0.017			
			4799	245.7	0.025
4584	143.0	0.006	**4578**	403.4	0.095
			4212	125.4	0.011
4180	163.0	0.044			
			4127	245.5	0.248
4102	103.6	0.010			

Table 4. Energy of $^5T_{2g} \rightarrow {}^5E_g$ transition and its splitting (cm^{-1}) of ferrous ion in selected iron(II) and iron(III) sulphate minerals

Mineral	Component band positions		Separation of the splitting	Crystal field strength (10Dq)
	1	2		
M30720 (Jarosite)	10650	10200	450	10425
M32767 (Pb-jarosite)	10560	9920	640	10240
M37059 (Romerite)	9800	8410	390	9105
M47134 (Parabutlerite)	9810	8435	375	9123
M34345 (Siderotil)	9985	8905	1080	9445

List of Figures

List of Tables

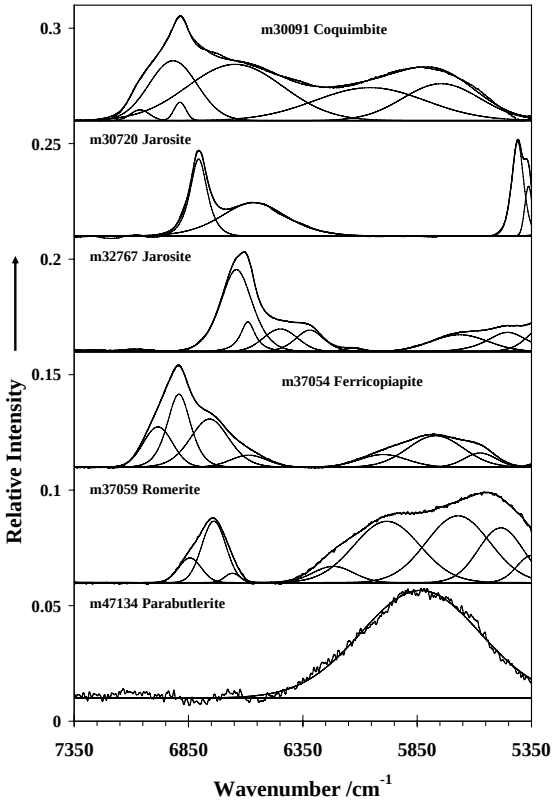
m30091 Coquimbite
m30720 Jarosite
m32767 Jarosite
m37054 Ferricopiapite
m37059 Romerite
m47134 Parabutlerite
Relative Intensity
0.3
0.25
0.2
0.15
0.1
0.05
0
7350
6850
6350
5850
5350
Wavenumber /cm-1

Figure 1

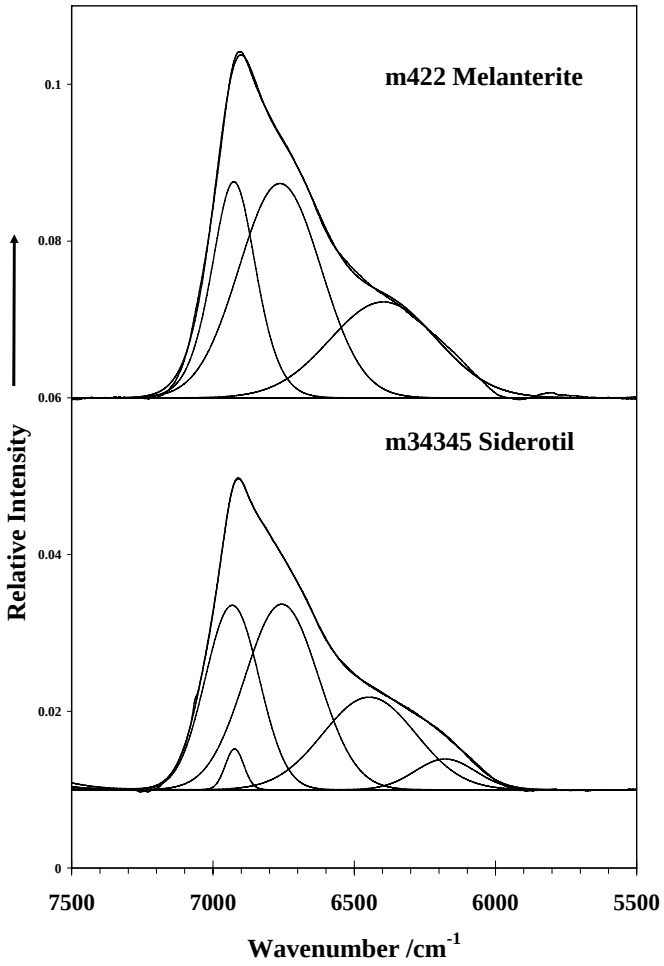
m422 Melanterite
m34345 Siderotil
Relative Intensity
0.1
0.08
0.06
0.04
0.02
0
7500
7000
6500
6000
5500
Wavenumber /cm-1

Figure 2

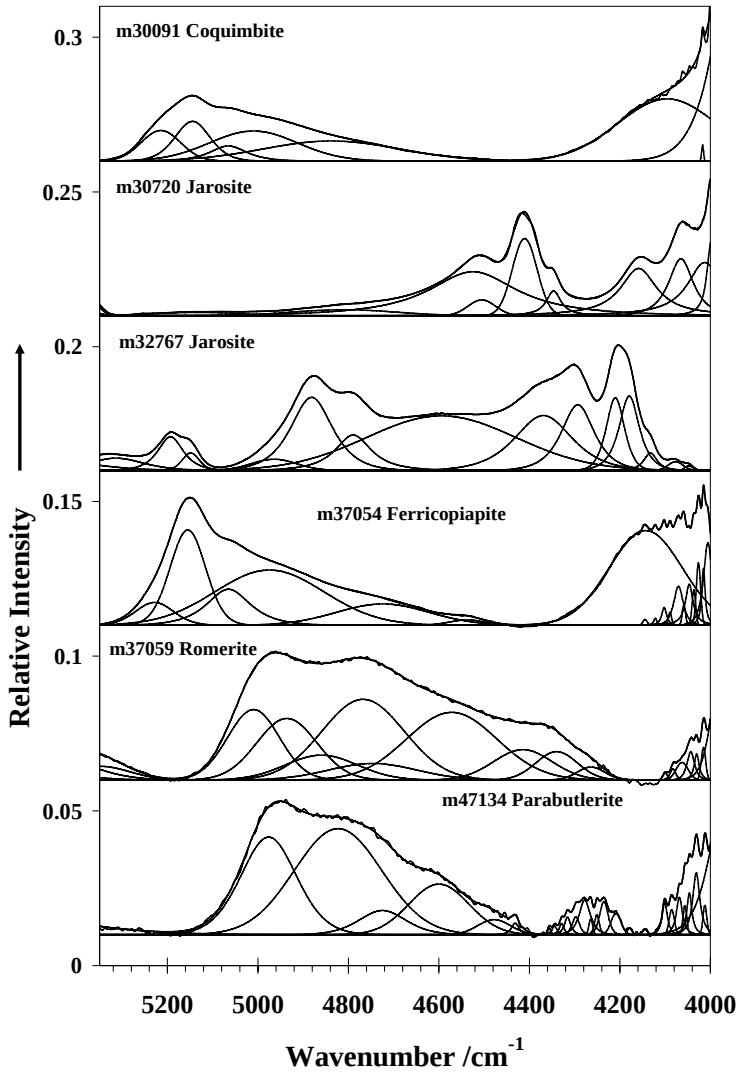
m30091 Coquimbite
m30720 Jarosite
m32767 Jarosite
m37054 Ferricopiapite
m37059 Romerite
m47134 Parabutlerite
Relative Intensity
0.3
0.25
0.2
0.15
0.1
0.05
0
5200
5000
4800
4600
4400
4200
4000
Wavenumber /cm-1

Figure 3

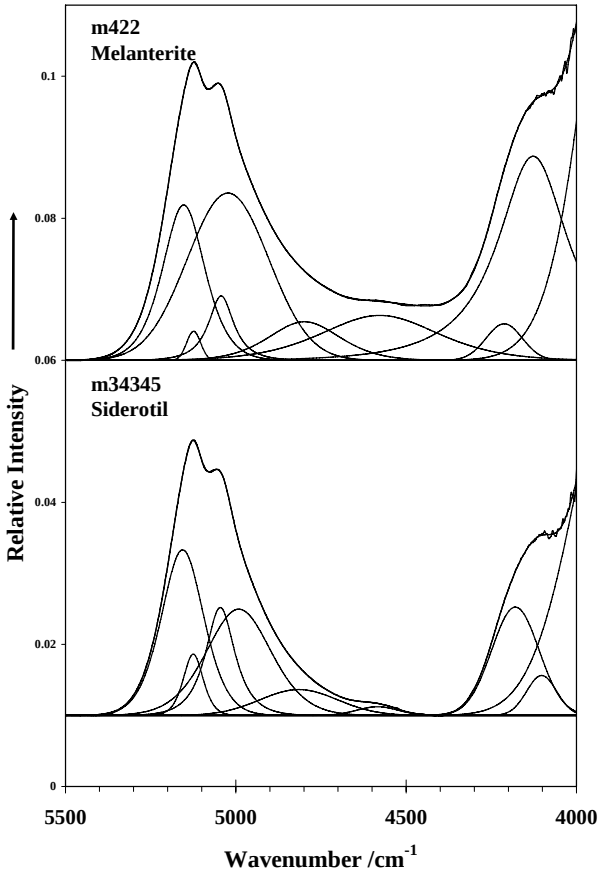
m422
Melanterite
m34345
Siderotil
Relative Intensity
0.1
0.08
0.06
0.04
0.02
0
5500
5000
4500
4000
Wavenumber /cm-1

Figure 4

Figure 5

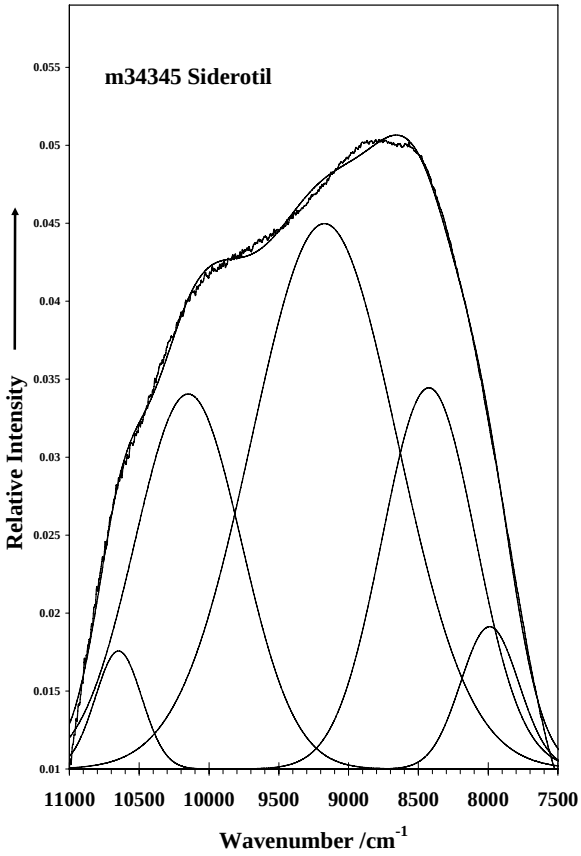

Figure 5

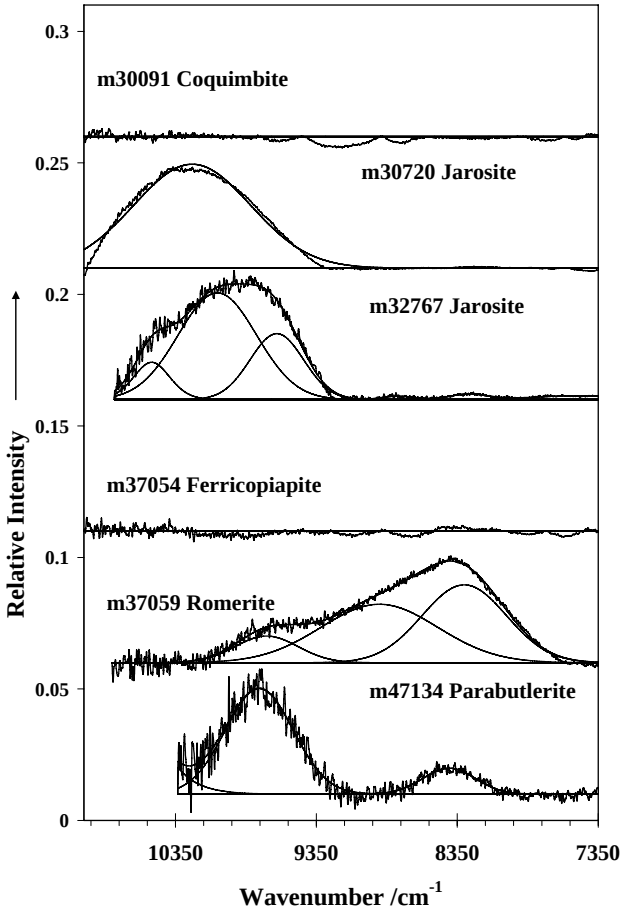
m30091 Coquimbite
m30720 Jarosite
m32767 Jarosite
m37054 Ferricopiapite
m37059 Romerite
m47134 Parabutlerite
Relative Intensity
0.3
0.25
0.2
0.15
0.1
0.05
0
10350
9350
8350
7350
Wavenumber /cm-1

Figure 6